

---

# **DATA PAPER**

## **A Subset of CyberShake Ground-Motion Time Series for Response-History Analysis**

Earthquake Spectra  
37(2) 1162-1176  
Author preprint version  
© The Authors 2021  
Reprints and permission:  
sagepub.co.uk/journalsPermissions.nav  
DOI: <https://doi.org/10.1177/8755293020981970>  
[www.sagepub.com/](http://www.sagepub.com/)

SAGE

<sup>2</sup> Jack W. Baker,<sup>1</sup> M.EERI, Sanaz Rezaeian,<sup>2</sup> Christine A. Goulet,<sup>3</sup>  
<sup>3</sup> M.EERI, Nicolas Luco,<sup>2</sup> M.EERI, and Ganyu Teng,<sup>1</sup> M.EERI

### **Abstract**

<sup>4</sup> This manuscript describes a subset of CyberShake numerically simulated ground motions that were selected and vetted for use in engineering response-history analyses. Ground motions were selected that have seismological properties and response spectra representative of conditions in the Los Angeles area, based on disaggregation of seismic hazard. Ground motions were selected from millions of available time series and were reviewed to confirm their suitability for response-history analysis. The processes used to select the time series, the characteristics of the resulting data, and the provided documentation are described in this manuscript. The resulting data and documentation are available electronically.

### **Keywords**

<sup>5</sup> CyberShake, Physics-Based Ground-Motion Simulations, Time Series, Response-History Analysis

---

<sup>1</sup> Stanford University, USA

<sup>2</sup> U.S. Geological Survey, USA

<sup>3</sup> University of Southern California and Southern California Earthquake Center, USA

### **Corresponding author:**

Jack Baker, Stanford University, 473 Via Ortega, MC 4020, Stanford, CA 94305, USA.

Email: [bakerjw@stanford.edu](mailto:bakerjw@stanford.edu)

## 6 Introduction

7 Numerical ‘physics-based’ simulations of ground motions are an increasingly valuable  
8 resource for engineers, and they play a role in both ground-motion hazard analysis and  
9 response-history analysis. Provided that the simulation methods and parameters have  
10 been properly validated in ranges for which recorded data exist, they can provide insight  
11 into the scaling of ground motions with magnitude and distance or for rupture geometries  
12 not yet observed. One other advantage of simulations versus recorded ground-motion  
13 data is the essentially infinite amount of variations that can be produced for a wide range  
14 of rupture and site characteristics. Conversely, the massive amount of potential data and  
15 variations to choose from can make it difficult for a structural design team to quickly  
16 locate appropriate time series for analysis.

17 This Data Paper aims to address the issue by documenting a subset of time series  
18 selected from the CyberShake platform output. A small number of time series (i.e.,  
19 320 two-component horizontal ground motions) were selected from rupture scenarios  
20 of interest for engineering analysis in southern California. They were screened to have  
21 suitable response spectra and vetted to omit time series with unusual or potentially  
22 problematic characteristics. This paper describes the project’s objectives and documents  
23 the process used to select the time series.

24 CyberShake is a Southern California Earthquake Center (SCEC) high-performance  
25 computing platform developed to conduct simulation-based seismic hazard analysis.  
26 It samples an earthquake rupture forecast (ERF) to generate earthquake ruptures, for  
27 which wave propagation is then computed (Graves et al. 2011; Jordan et al. 2018;  
28 SCECpedia 2020). The CyberShake products include ground-motion time series and  
29 intensity measures at selected sites on a closely spaced grid. The current implementation  
30 of CyberShake uses the Uniform California Earthquake Rupture Forecast 2 (UCERF2,  
31 Field et al. 2009) and samples over 400,000 ruptures from the model, focusing on  
32 Moment Magnitudes ( $M$ ) of 6 and above, within 200 km of a site. Earthquake ruptures  
33 are described kinematically, with slip amplitude, direction, and timing across the fault  
34 specified based on models calibrated from inversions of past earthquake sources and  
35 dynamic rupture simulations (Graves and Pitarka 2015). The CyberShake platform uses  
36 reciprocity to compute wave propagation through Green strain tensors computed for  
37 three-dimensional (3D) velocity models of the Earth, which incorporate the effects of  
38 sedimentary basins and other features in the crust. Because these simulations reflect  
39 the physical processes associated with earthquake rupture and wave propagation, they  
40 and other similar approaches are often referred to as ‘physics-based.’ CyberShake Study  
41 15.12 results used here also include stochastically simulated high-frequency ( $> 1$  Hz)  
42 ground motion in addition to the deterministic low-frequency simulations described  
43 above. The high-frequency simulation uses a physically motivated but simplified model  
44 for wave propagation and scattering to generate theoretically consistent ground motion  
45 amplitudes at these frequencies, based in part on the model of Boore (1983). Because  
46 explicit wave propagation simulation at high frequencies would require source and  
47 crustal properties that are unknown, this stochastic approach is a viable method to obtain  
48 a more realistic ground motion across the full frequency range of interest. The resulting

49 ground motions are expected to exhibit realistic features for frequencies that are of most  
 50 interest for engineering analysis (up to about 20 Hz). The implementation of this hybrid  
 51 approach follows that described in Graves and Pitarka (2010).

52 The region of interest for this study is the greater Los Angeles area (Figure 1). The 3D  
 53 velocity model used for this CyberShake region (CVM-S4.26.M01) has been validated  
 54 for the ground motions it produced by different teams of researchers using waveforms  
 55 and various engineering metrics (e.g., Lee and Chen 2016; Small et al. 2017; Taborda  
 56 et al. 2016). Simulations from the CyberShake platform (ruptures, velocity model, wave  
 57 propagation) have been used previously for estimating response spectra for seismic  
 58 design (Crouse and Jordan 2016; Crouse et al. 2018) and for response-history analysis  
 59 and validation (Bijelić et al. 2019a,b; Teng and Baker 2019).

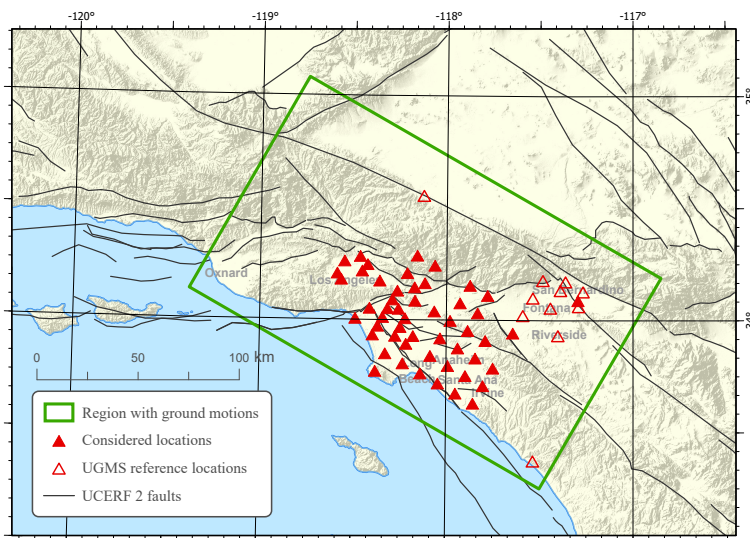


**Figure 1.** Map of the study area, showing the CyberShake simulation domain, the considered candidate locations and the earthquake sources (UCERF2 faults).

60 Ground-motion simulations can be used for several purposes in engineering analyses  
 61 (Bradley et al. 2017), including response history analysis, supporting the development of  
 62 empirically-calibrated Ground-Motion Models (GMMs), or hazard analysis to estimate  
 63 ground shaking amplitudes or structural responses from future earthquakes. In particular,  
 64 seismic hazard analysis can be advanced by utilizing simulations to supplement  
 65 predictions from empirically-calibrated GMMs because simulations can be produced for  
 66 areas with limited empirical data from ground motion recording typically used for hazard  
 67 analysis (Dreger et al. 2015; Goulet et al. 2015). Simulations present an advantage over  
 68 GMMs in that they produce complete time series, not only spectral response.

69 Hence, given a hazard analysis and target spectrum, simulated ground-motion time  
 70 series can be used as inputs to a response-history analysis. To date, engineering analysis  
 71 studies have found that the CyberShake ground motions generally have realistic features

of engineering interest and that basin effects may, in some cases, produce greater structural demands than comparable recordings with no basin effects (Bijelić et al. 2019b). This motivates our desire to provide time series from this platform for engineers needing to consider such effects.

When performing ground-motion selection for this effort, we took the perspective of an engineering consultant looking to utilize ground motions for a design or assessment project in the Los Angeles area. In projects requiring time series for response-history analysis, a site-specific spectrum (or spectra) will be utilized, considering site conditions and other unique features of a given site (e.g. ASCE 2016; LATBSDC 2008; Moehle et al. 2017). Furthermore, future projects could take place at many locations. Hence, we did not define a single location or target spectrum for this project, and we determined that it would be best to select ground motions with a range of spectral amplitudes and shapes for that relatively large region. Most consultants are accustomed to simple interfaces to existing libraries of recorded ground motions and may find the SQL-based CyberShake interface challenging. Additionally, considering more than 159 million available two-component seismograms is much more complicated than selecting from amongst a few thousand recordings. These considerations were the primary motivation behind our work. By pre-screening and pre-vetting a manageable subset of ground motions, we add value to an engineering consultant who may not have prior experience reviewing ground-motion simulations and may need to justify the quality of the motions to a peer review panel and other members of the project team. The selected ground motions also supplement existing recorded datasets in a meaningful way as they span magnitude and distance ranges currently poorly represented. These ground motions also include the regional crustal effects expected in the Los Angeles area.

## Ground-Motion Selection Approach

The process used to select the ground motions consisted of the following steps, which are described in the following subsections:

1. Specify candidate locations and site conditions of interest.
2. Perform hazard disaggregation for cases of interest to determine earthquake scenarios (i.e., magnitudes and distances) contributing most to hazard.
3. Select a small number of target earthquake scenarios based on disaggregation data and screen the CyberShake database to find simulations from those scenarios.
4. Generate target response spectra for each target earthquake scenario and select closely matching recordings from the screened database.
5. Review the identified time series.
6. Produce documentation.

### *Specify Candidate Locations and Site Conditions*

We considered 52 locations in a Los Angeles region, as shown in Figure 1. These locations are a subset of the 63 reference locations previously used by the SCEC Utilization of Ground Motion Simulations (UGMS) committee (<https://data2.>

**Table 1.** Example disaggregation results for a location near downtown Los Angeles. Sources contributing more than 1% to exceedances of the  $SA(1s)$   $MCE_R$  amplitude are listed, along with their percent contribution, and mean values of magnitude and distance. Distance is defined as the closest distance to the rupture.

Source	Contribution [%]	Magnitude	Distance [km]
Elysian Park	30.9	6.9	5.4
Puente Hills	16.0	7.2	6.6
Newport-Inglewood	9.7	7.3	13.1
Compton	8.3	7.3	14.5
Background seismicity	6.8	6.4	8.6
Hollywood	4.7	7.3	8.3
San Andreas	3.0	8.1	55.5
Sierra Madre	2.7	7.7	19.9
San Vicente	1.2	6.7	6.3

112 [seec.org/ugms-mcerGM-tool\\_v18.4/](https://seec.org/ugms-mcerGM-tool_v18.4/), Crouse et al. 2018), selected from the  
 113 available 336 sites in CyberShake study 15.12. The subset includes locations where the  
 114 U.S. Geological Survey (USGS) had previously performed disaggregations on a tightly-  
 115 spaced grid (0.01 by 0.01 degree).

### 116 *Perform Hazard Disaggregation*

117 For each of the locations and site conditions, disaggregation was performed to identify the  
 118 earthquake magnitudes and distances most likely to cause ground-motion amplitudes of  
 119 engineering interest. Hazard and disaggregation calculations from the most recent USGS  
 120 National Seismic Hazard Model (Petersen et al. 2020) were used for these evaluations.  
 121 The ground-motion amplitudes of interest were pseudo-spectral acceleration ( $SA$ ) values  
 122 at risk-targeted Maximum Considered Earthquake ( $MCE_R$ ) amplitudes, as computed for  
 123 the 2020 NEHRP Recommended Seismic Provisions (Hamburger et al. 2017).

124 Disaggregation was initially performed at 22 spectral periods from 0 to 10 s and for  
 125 eight of the site classes defined by the 2020 NEHRP Recommended Seismic Provisions.  
 126 Based on an evaluation of those data, the analysis was simplified to consider two site  
 127 condition values ( $V_{S,30} = 365$  and  $760$  m/s), and four spectral periods (0.2, 1, 2, and 5  
 128 seconds), as those were seen to produce disaggregation results representative of the other  
 129 conditions as well.

130 Each disaggregation calculation produced a list of fault sources that significantly  
 131 contributed to the total hazard, with respective mean earthquake magnitudes and mean  
 132 source-to-site distances. Table 1 shows sample results from a location in downtown Los  
 133 Angeles (latitude =  $34.05$ , longitude =  $-118.25$ ), a  $V_{S,30}$  of  $365$  m/s, and a spectral period  
 134 of 1 second.

135 The magnitude and distance values for all locations, periods, and site conditions  
 136 are shown in Figure 2. As expected, the  $MCE_R$  amplitudes for all cases result from  
 137 large magnitude ruptures at small distances. In contrast, the vast majority of available  
 138 ground-motion recordings are from smaller magnitude and larger source-site distances.

139 To illustrate, the magnitude and distance values of recordings available in the large  
 140 NGA-West2 ground-motion database (Ancheta et al. 2014) are also shown in Figure 2.  
 141 The relative sparsity of available recordings with target magnitude and distance values  
 142 motivates the collection of the simulations described herein.

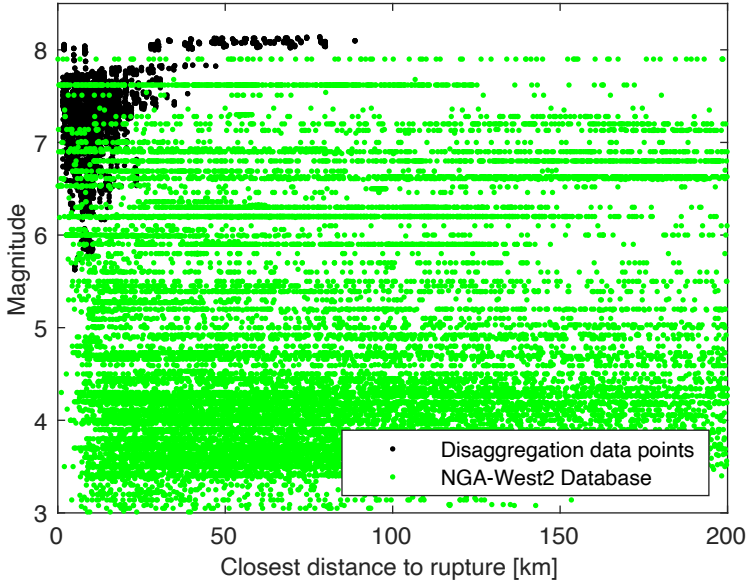


**Figure 2.** Magnitude and distance values of disaggregation targets from this study, and of ground motions in the NGA-West2 database (Ancheta et al. 2014).

143 Figure 3 shows disaggregation results for particular site conditions and spectral periods  
 144 to illustrate key patterns in the results. To account for the fact that each point on the plots  
 145 has a different percent contribution, we performed a kernel-smoothed estimate of the total  
 146 contributions associated with each magnitude and distance value. At each magnitude and  
 147 distance value, all points within  $\pm 0.2$  magnitude units and  $\pm 5$  km were collected, and  
 148 the sum of the percent contributions was computed. Contours of these resulting estimates  
 149 are shown in the figure to indicate the magnitude and distance values most likely to be  
 150 contributing to hazard.

151 Several observations can be made from Figure 3. The similarity of Figure 3a and  
 152 3b, which consider the same periods but differing site conditions, confirms that site  
 153 conditions have a negligible impact on the disaggregation result of interest. Given this  
 154 stable disaggregation result, we use the same rupture scenarios for both site conditions.  
 155 A comparison of Figure 3c and d, which have the same site conditions but consider  
 156 short- and long-period  $SA$  values, shows that the short-period  $SA$  values are mostly  
 157 caused by moderate-magnitude ( $5.5 < M < 7.5$ ) earthquakes at distances within 20 km.

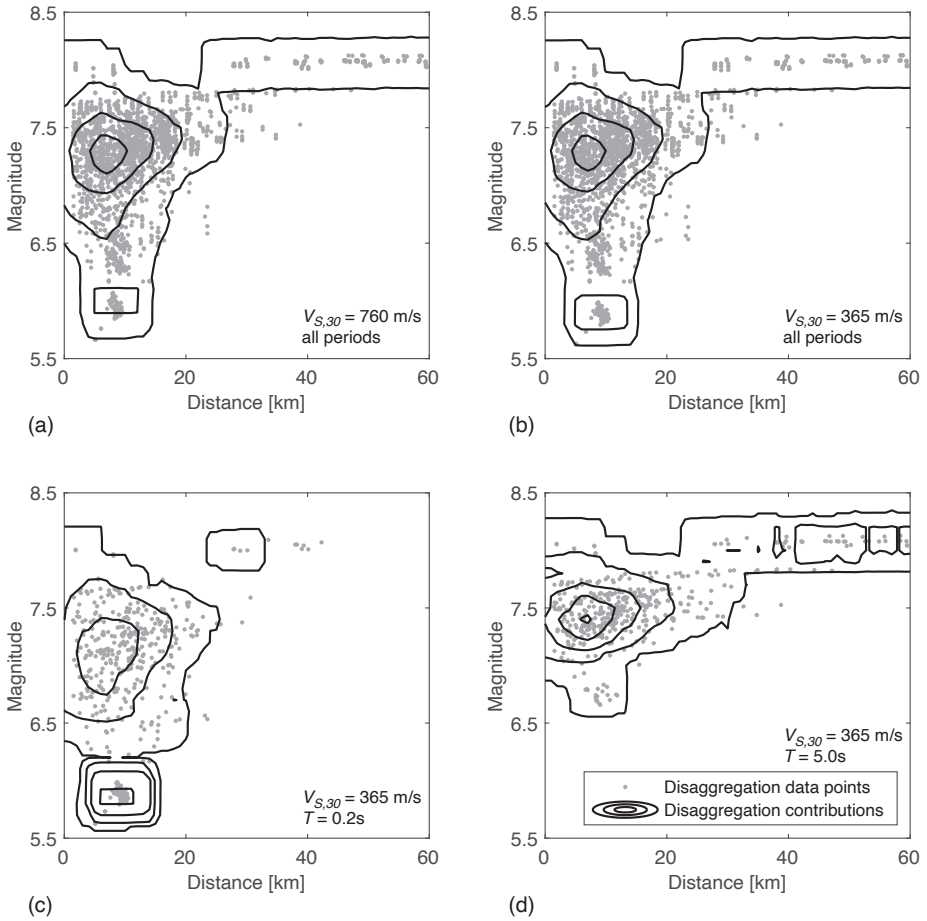


**Figure 3.** Disaggregation values for subsets of cases. Black lines show contours from kernel smoothing (values within  $\pm 0.2$  magnitude units and  $\pm 5$  km), to indicate magnitudes and distances with highest disaggregation contributions. (a)  $V_{S,30} = 760$  m/s, all periods. (b)  $V_{S,30} = 365$  m/s, all periods. (c)  $V_{S,30} = 365$  m/s,  $T = 0.2$ s. (d)  $V_{S,30} = 365$  m/s,  $T = 5.0$ s.

158 In contrast, longer-period  $SA$  values are more likely to be caused by larger-magnitude  
 159 and more distant ruptures.

### 160 *Select Rupture Scenarios and Screen Database*

161 Because the selected ground motions are intended to be relevant for a range of locations,  
 162 site conditions, and spectral periods, the disaggregation data were pooled and used to  
 163 select representative rupture scenarios (Figure 4). We focused on scenarios that appear  
 164 frequently in the disaggregation data and where few recordings are available. Figure 4

165 shows the selected target scenarios. Magnitude 8 ruptures at distances of 5 and 40 km  
 166 were selected to represent large magnitude events that could produce expected long-  
 167 duration shaking. Magnitude 7.3 and 6.5 ruptures at distances of 8 km were selected due  
 168 to the significant contribution they make to  $MCE_R$  hazard. Magnitude 6 ruptures at 10  
 169 km also make a significant contribution to hazard, but they were not considered further  
 170 as many suitable ground-motion recordings exist for this case (Figure 2).

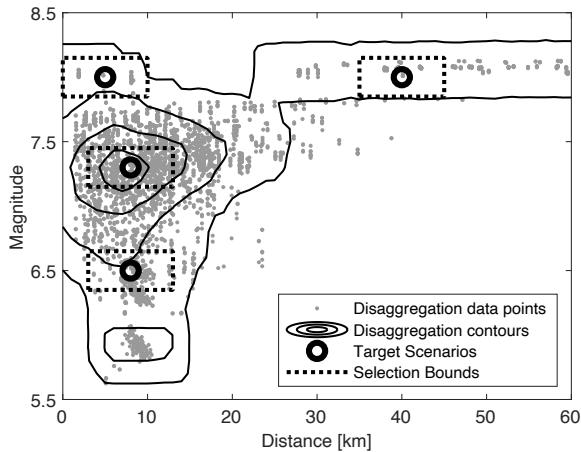


**Figure 4.** Disaggregation values for all cases (grey dots), contours from kernel smoothing (black lines), target earthquake scenarios (black circles), and bounds around the scenarios for selection (dotted black lines).

171 For each of these four rupture scenarios, and for each of the two site conditions, we  
 172 search the CyberShake database for time series associated with these conditions. Because  
 173 our selected rupture scenarios and site conditions are intended to represent a range  
 174 of similar conditions rather than a precise magnitude, distance, and  $V_{S,30}$ , a range of  
 175 acceptable values were considered for each case. The ranges deemed to produce suitable  
 176 numbers of ground motions and cover the rupture conditions of interest were  $M \pm 0.15$ ,  
 177  $R \pm 5$  km, and  $V_{S,30} \pm 20$  m/s. Figure 4 shows the bounds of these selection criteria  
 178 around each of the four scenarios. The ranges of considered parameter values are quite  
 179 narrow compared to typical ranges used in selection of recorded ground motions because  
 180 of the large number of available simulations as discussed in the following paragraph.  
 181 The magnitude range is one exception—this is somewhat wider because the simulated  
 182 magnitudes are discretized at intervals of 0.1, so a wider range is needed to include these  
 183 discrete values.

184 The number of CyberShake time series matching these selected ranges are shown in  
 185 Table 2. In contrast to databases of recorded ground motions, where there are often few  
 186 if any suitable recordings, there are tens of thousands of available simulated time series  
 187 for each rupture scenario of interest. Also in contrast to databases of recorded ground  
 188 motions, the most time series are available for the largest-magnitude scenarios. This is

**Table 2.** Number of available Cybershake time series for each of the eight scenarios of interest. The left three columns specify the scenario, the fourth column indicates the number of ruptures and corresponding sites matching the scenario, and the fifth column indicates the number of available time series.

Magnitude	Distance (km)	$V_{S,30}$ (m/s)	# of site-rupture pairs	# of ground motions
8.0	5	760	5,553	2,075,381
8.0	5	365	2,444	904,177
8.0	40	760	2,031	725,068
8.0	40	365	890	311,188
7.3	8	760	4,847	511,899
7.3	8	365	2,166	233,708
6.5	8	760	1,904	33,487
6.5	8	365	943	16,445

189 because the CyberShake platform is designed to produce more rupture realizations for  
 190 ruptures with a large surface area, which is correlated with magnitude.

### 191 *Generate Target Response Spectra and Select Matching Motions*

192 Simply constraining the rupture and site characteristics for ground-motion selection  
 193 leaves millions of available candidate time series, as seen in Table 2. That is many more  
 194 than are needed for engineering evaluations considered by this project. To further reduce  
 195 the selected set of motions, while ensuring that the chosen motions have ‘useful’ levels  
 196 of shaking amplitude, a spectral-target-based selection approach was utilized. The use of  
 197 a spectrum for this step is a means to an end to reduce the large dataset and to eliminate  
 198 time series that diverge significantly from a typical spectral shape.

199 The procedure used at this step is illustrated in Figure 5. For each rupture scenario, the  
 200 means, standard deviations, and period-to-period correlations of resulting (log) response  
 201 spectra are computed from empirical ground-motion models (Baker and Jayaram 2008;  
 202 Boore et al. 2014). Then samples of response spectra are generated using a Monte Carlo  
 203 simulation, assuming that the log response spectra have a multivariate normal distribution  
 204 with means, standard deviations, and correlations as computed in the previous step (from  
 205 the empirical datasets). Finally, each of the sampled response spectra is compared to  
 206 the available ground motions’ response spectra, and the ground motion with the closest  
 207 match is selected. This process follows the ‘unconditional selection’ algorithm that has  
 208 been previously applied to select ground motions from databases of recordings (Baker  
 209 et al. 2011).

210 The proposed procedure has several advantages for this application. First, the process  
 211 of matching to spectra ensures that the amplitudes of the selected simulations are  
 212 consistent with empirical data; hence, any simulations with unexpected amplitudes are  
 213 not selected. There is a broader academic question as to whether simulated amplitudes  
 214 that meaningfully differ from empirical models indicate a deficiency in empirical models.  
 215 For this application, however, we are assuming that the target amplitudes are coming from  
 216 other sources and that the simulations are not being utilized to question those amplitudes.  
 217 Second, the process results in a set of ground motions whose spectra cover a range of

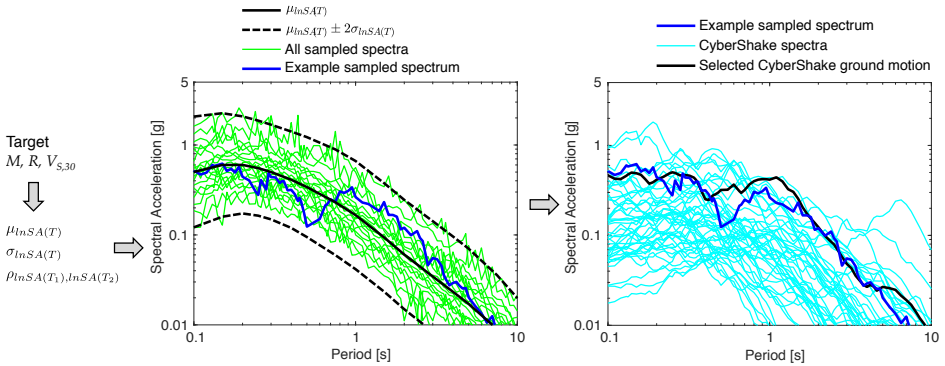


**Figure 5.** Schematic illustration of the ground-motion selection process. We first specify a target scenario and compute the means, standard deviations and correlations of  $lnSA$  (left); we then sample response spectra from the resulting distribution (middle); finally, we compare each sampled response spectrum to the CyberShake spectra and select the closest match (right).

218 plausible amplitudes and shapes (e.g., Figure 6). We have not pre-assumed a specific  
 219 design spectrum, so a user with an arbitrary spectrum can find suitable ground motions  
 220 in this set. Third, the process can produce an arbitrary number of selected motions, simply  
 221 by varying the number of Monte Carlo samples.

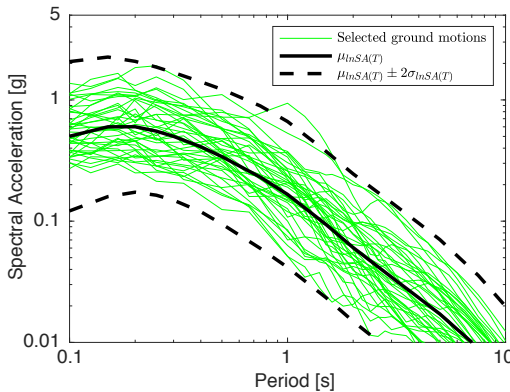


**Figure 6.** Response spectra of CyberShake ground motions selected to match the  $M = 6.5$ , distance = 8 km,  $V_{S,30} = 760$  m/s scenario. Mean and mean  $\pm$  2 standard deviation predictions of  $lnSA$  for that scenario are superimposed for reference.

222 For this particular application, the following choices were made when implementing  
 223 the sampling and selection algorithm.

- The models of Boore et al. (2014) and Baker and Jayaram (2008) were used to generate the target mean, standard deviation, and correlation values for the Monte Carlo simulations.
- Thirty spectral acceleration periods between 0.1 and 10 seconds were considered when sampling spectra and comparing simulations to these samples. The periods were those for which spectral values are tabulated in the CyberShake database. While longer periods are presumably of greatest interest given the intended application to tall buildings, and given that the simulations produce the most insight at long periods, all periods were considered at this step because it was not difficult to obtain time series with appropriate spectra over the full period range.
- Forty Monte Carlo samples of response spectra were produced for each of the eight scenarios, and one CyberShake ground motion was selected to match each sample.
- RotD50 response spectra were used for both the target spectra sampling and the CyberShake simulation spectra. This is the median spectral amplitude over all possible horizontal orientations of the ground motion (Boore 2010). (The RotD100 spectra of the selected ground motion motions are also consistent with anticipated spectral amplitudes, and either metric could have been used at this step without significant impact on the results.)
- The match between a sampled target spectrum and a particular simulation was measured using the sum of squared errors between the log sampled spectrum and log CyberShake spectrum, over the 30 periods of interest.
- No amplitude scaling of the ground motions was permitted.
- Selected ground motions consist of the two horizontal components for which the RotD50 values were screened. Vertical ground motions are not produced in this simulation platform, and so are not provided.

Example response spectra of ground motions selected by this process are shown in Figure 6. We note that the variability of these selected spectra is slightly lower than the variability of the initial target response spectra. This is partly due to the spectral shapes of ground motions available in the CyberShake database, and these differences are visually exacerbated in Figure 6 because spectral values are plotted for a relatively small number of periods. This is acceptable, as the goal is not to perfectly replicate the distribution of spectral values predicted by a ground-motion model, but rather to provide the engineering community with ground motions exhibiting reasonable and defensible amplitudes and a range of spectral shapes. Trial efforts to select ground motions from the developed subset indicates that it is feasible to select motions matching a range of conditional mean spectral shapes and other potential target spectra; hence, the results were deemed satisfactory.

Figure 7 compares response spectral values of the selected ground motions and the NGA West2 motions. Figure 7a shows response spectra of a random sample of 100 ground motions from each set. Figure 7b shows the complete sets of ground motions, plotted for two spectral acceleration periods. The figure illustrates that the selected motions are comparably high in amplitude to (but not above) the strongest motions in the NGA West2 database, as anticipated from Figure 2.

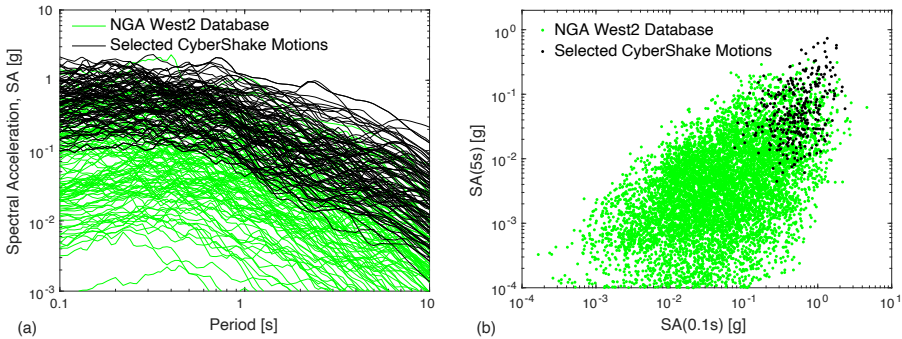


**Figure 7.** (a) Response spectra of 100 randomly selected ground motions with  $M > 5$  from the NGA West2 database, and 100 randomly selected ground motions from the curated set of CyberShake ground motions. (b) SA(0.1s) and SA(5s) values from the PEER NGA West2 database and the selected CyberShake ground motions.

## 267 *Review time series*

268 The process and results described above were subject to several stages of review during  
 269 the project. The candidate locations, disaggregation parameters and results, and selected  
 270 target earthquake scenarios were presented to the SCEC Ground Motion Simulation  
 271 Validation (GMSV) committee for comment and feedback. Once the target scenarios  
 272 were finalized, the ground-motion selection process and selected ground motions were  
 273 presented to the GMSV committee and some members of the SCEC UGMS committee,  
 274 for further comment. Reviewed materials included plots of time series, response spectra,  
 275 and metadata for selected motions. These reviews (along with many iterations of internal  
 276 review by the authors), resulted in refinements to the analysis process, adjustments to the  
 277 selected set of ground motions, and identification of key metrics to document.

278 These reviews were intended to maximize the value of the final ground motion set and  
 279 also to encourage questions and potential objections that might arise if these data were  
 280 to be used in an engineering assessment. Based on the scrutiny that the ground motions  
 281 have received, and the lack of remaining concerns, we believe that these ground motions  
 282 would be suitable for use in response-history analysis applications as a supplement to or  
 283 in place of recordings.

## 284 *Produce Documentation and Repository*

285 The data repository is available at [https://doi.org/10.5281/zenodo.](https://doi.org/10.5281/zenodo.3875541)  
 286 3875541 (Baker et al. 2020a). The repository contains a Comma-Separated Values  
 287 (CSV) file with the following metadata fields for each selected ground motion:

- 288 • Station name and ID
- 289 • Site  $V_{S,30}$  (average shear wave velocity in the top 30m)
- 290 • Shortest distance to the rupture

- 291 ● Earthquake source name
- 292 ● Earthquake magnitude
- 293 ● An indicator of the presence of a velocity pulse, and the period of that pulse if it is
- 294 present (Shahi and Baker 2014)
- 295 ● 5-75% significant duration
- 296 ● Hypocenter latitude
- 297 ● Hypocenter longitude
- 298 ● Hypocenter depth
- 299 ● Depth to top of rupture
- 300 ● 5%-damped RotD50 response spectra at 30 periods between 0.1 and 10 seconds
- 301 ● File names for each component of the time series

302 Numerical data for each component of the time series are provided as individual text files.  
303 Finally, plots of response spectra and time series (acceleration, velocity, displacement)  
304 are provided for each ground motion component as individual Portable Network Graphic  
305 (PNG) files, and all of the figures are compiled into a summary Portable Document  
306 Format (PDF) report. Figure 8 shows example plots for one selected ground motion. The  
307 intended use of this repository is that a user can search the metadata file to find ground  
308 motions satisfying the desired selection criteria and then extract the corresponding time  
309 series files for further analysis.

310 The data are also loaded into a ground-motion selection tool at [https://github.com/bakerjw/CS\\_Selection](https://github.com/bakerjw/CS_Selection) (Baker et al. 2020b), so that the ground motions  
311 can easily be searched using the same approach as is available for searching libraries  
312 of recordings (Baker and Lee 2018).  
313

## 314 Conclusions

315 This paper summarizes the contents of a selected set of CyberShake ground motions,  
316 which were developed to facilitate the response-history analysis of structures. The  
317 CyberShake ground-motion database provides a library of millions of numerically  
318 simulated ground motions from large shallow crustal ruptures relevant for engineering  
319 analysis in Southern California. The CyberShake simulations also consider several  
320 physical processes of interest in Southern California, such as the effects of rupture  
321 directivity and sedimentary basins on shaking time series.

322 To utilize this extensive library for engineering analysis purposes, we developed a  
323 procedure to screen and select a small number of relevant ground motions. We performed  
324 seismic hazard disaggregation analysis for a number of Southern California locations to  
325 determine the earthquake ruptures that contribute most significantly to hazard. We then  
326 selected four target rupture scenarios and two near-surface soil conditions for each. For  
327 each scenario, we computed response spectra means, variances, and correlations from  
328 an empirical GMM and then generated corresponding Monte Carlo samples of response  
329 spectra. Those samples were used as targets to find CyberShake ground motions with  
330 comparable response spectra. This procedure resulted in a set of 320 ground motions  
331 (selected from a database of millions) that come from earthquake ruptures of interest to

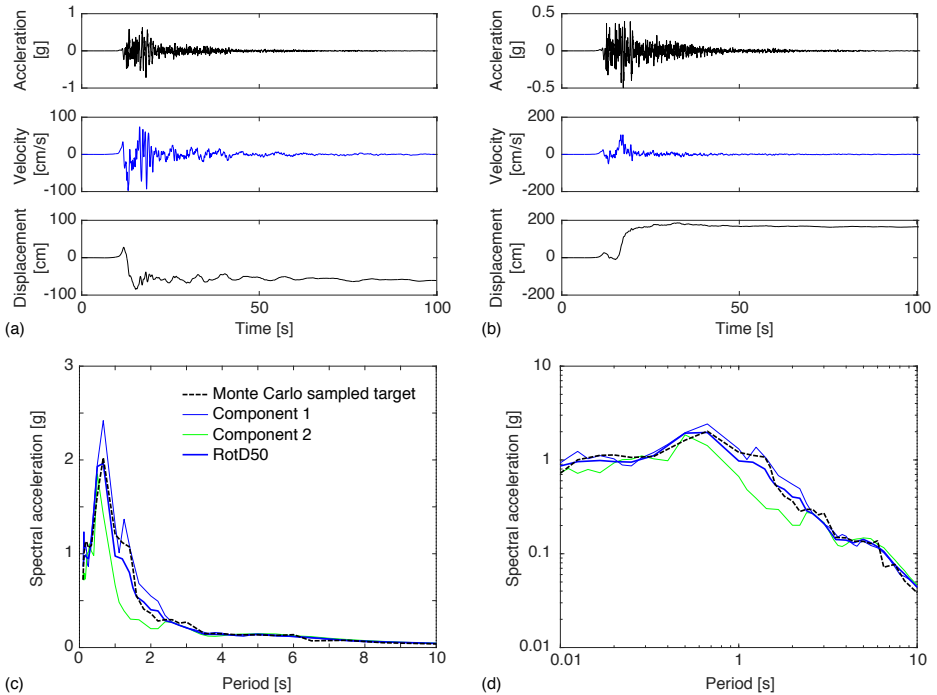


**Figure 8.** Example time series and spectra plots for a selected ground motion (a  $M = 7.85$  San Andreas rupture recorded at a distance of 0.3 km with  $V_{S,30} = 748$  m/s). (a) Component 1 acceleration, velocity and displacement. (b) Component 2 acceleration, velocity and displacement. (c) Response spectra in linear scale. (d) Response spectra in log scale.

332 engineers and that have realistic and defensible ground-motion amplitudes and spectral  
 333 shapes.

334 The resulting selected ground motions have also been reviewed to check for anomalous  
 335 features or characteristics that might make them questionable. We believe that the  
 336 resulting set of ground motions are appropriate for use in response-history analysis  
 337 of structures and that the pre-screening and review make the dataset more practical  
 338 for engineers than the complete original database. The process utilized here can be  
 339 replicated in the future, as ground-motion simulation databases become increasingly  
 340 large, necessitating procedures to screen and select appropriate subsets of ground  
 341 motions.

## 342 Acknowledgements

343 We thank Scott Callaghan for help in accessing the CyberShake database, Edric Pauk and Tran  
 344 Huynh for helping host these data, N. Simon Kwong for testing and improving the ground-motion  
 345 selection data, and Brendon Bradley and Rob Graves for helpful feedback on the draft manuscript.

346 We thank the SCEC Ground Motion Simulation Validation (GMSV) and Utilization of Ground  
347 Motions (UGMS) committees for helpful feedback throughout this effort, which increased the  
348 utility of the final product.

## 349 Funding

350 This research was supported by the Southern California Earthquake Center (Contribution No.  
351 10077). SCEC is funded by NSF Cooperative Agreement EAR-1033462 & USGS Cooperative  
352 Agreement G12AC20038.

## 353 References

- 354 Ancheta TD, Darragh RB, Stewart JP, Seyhan E, Silva WJ, Chiou BJS, Wooddell KE, Graves RW,  
355 Kottke AR, Boore DM, Kishida T and Donahue JL (2014) NGA-West2 database. *Earthquake*  
356 *Spectra* 30(3): 989–1005. DOI:10.1193/070913EQS197M.
- 357 ASCE (2016) *Minimum Design Loads for Buildings and Other Structures, ASCE 7-16*. ASCE/SEI  
358 7-16. Reston, Virginia: American Society of Civil Engineers/Structural Engineering Institute.
- 359 Baker JW, Goulet C, Luco N, Rezaeian S and Teng G (2020a) A subset of CyberShake ground  
360 motion time series for response history analysis. *Zenodo* (Version 1.0.1). DOI:10.5281/  
361 zenodo.3922295.
- 362 Baker JW and Jayaram N (2008) Correlation of spectral acceleration values from NGA ground  
363 motion models. *Earthquake Spectra* 24(1): 299–317. DOI:10.1193/1.2857544.
- 364 Baker JW and Lee C (2018) An improved algorithm for selecting ground motions to match a  
365 conditional spectrum. *Journal of Earthquake Engineering* 22(4): 708–723. DOI:10.1080/  
366 13632469.2016.1264334.
- 367 Baker JW, Lee C and Kwong NS (2020b) Bakerjw/cs\_selection: Added cybershake database.  
368 *Zenodo*. DOI:10.5281/zenodo.4042691.
- 369 Baker JW, Lin T, Shahi SK and Jayaram N (2011) New ground motion selection procedures  
370 and selected motions for the peer transportation research program. PEER Technical Report  
371 2011/03.
- 372 Bijelić N, Lin T and Deierlein GG (2019a) Evaluation of building collapse risk and drift demands  
373 by nonlinear structural analyses using conventional hazard analysis versus direct simulation  
374 with CyberShake seismograms. *Bulletin of the Seismological Society of America* 109(5):  
375 1812–1828. DOI:10.1785/0120180324.
- 376 Bijelić N, Lin T and Deierlein GG (2019b) Quantification of the influence of deep basin  
377 effects on structural collapse using SCEC CyberShake earthquake ground motion simulations.  
378 *Earthquake Spectra* 35(4): 1845–1864. DOI:10.1193/080418EQS197M.
- 379 Boore DM (1983) Stochastic simulation of high-frequency ground motions based on seismological  
380 models of the radiated spectra. *Bulletin of the Seismological Society of America* 73(6A): 1865–  
381 1894. December 1, 1983.
- 382 Boore DM (2010) Orientation-independent, nongeometric-mean measures of seismic intensity  
383 from two horizontal components of motion. *Bulletin of the Seismological Society of America*  
384 100(4): 1830–1835. DOI:10.1785/0120090400.

- 385 Boore DM, Stewart JP, Seyhan E and Atkinson GM (2014) NGA-West2 equations for predicting  
386 PGA, PGV, and 5% damped PSA for shallow crustal earthquakes. *Earthquake Spectra* 30(3):  
387 1057–1085. DOI:10.1193/070113EQS184M.
- 388 Bradley BA, Pettinga D, Baker JW and Fraser J (2017) Guidance on the utilization of earthquake-  
389 induced ground motion simulations in engineering practice. *Earthquake Spectra* 33(3): 809–  
390 835. DOI:10.1193/120216EQS219EP.
- 391 Crouse CB and Jordan TH (2016) Development of new ground-motion maps for Los Angeles  
392 based on 3-d numerical simulations and NGA West2 equations. In: *Proceedings of the SMIP17*  
393 *Seminar on Utilization of Strong Motion Data*.
- 394 Crouse CB, Jordan TH, Milner KR, Goulet CA, Callaghan S and Graves RW (2018) Site-specific  
395 MCER response spectra for Los Angeles region based on 3-d numerical simulations and the  
396 NGA West2 equations. In: *11th National Conference in Earthquake Engineering*, volume 518.  
397 Los Angeles, California, USA.
- 398 Dreger DS, Beroza GC, Day SM, Goulet CA, Jordan TH, Spudich PA and Stewart JP (2015)  
399 Validation of the SCEC broadband platform v14.3 simulation methods using pseudospectral  
400 acceleration data. *Seismological Research Letters* 86(1): 39–47. DOI:10.1785/0220140118.
- 401 Field EH, Dawson TE, Felzer KR, Frankel AD, Gupta V, Jordan TH, Parsons T, Petersen MD,  
402 Stein RS, Weldon RJ and Wills CJ (2009) Uniform California Earthquake Rupture Forecast,  
403 version 2 (UCERF 2). *Bulletin of the Seismological Society of America* 99(4): 2053–2107.  
404 DOI:10.1785/0120080049.
- 405 Goulet CA, Abrahamson NA, Somerville PG and Wooddell KE (2015) The SCEC broadband  
406 platform validation exercise: Methodology for code validation in the context of seismic-hazard  
407 analyses. *Seismological Research Letters* 86(1): 17–26. DOI:10.1785/0220140104.
- 408 Graves R, Jordan TH, Callaghan S, Deelman E, Field E, Juve G, Kesselman C, Maechling P, Mehta  
409 G, Milner K et al. (2011) CyberShake: A physics-based seismic hazard model for southern  
410 california. *Pure and Applied Geophysics* 168(3–4): 367–381.
- 411 Graves R and Pitarka A (2015) Refinements to the Graves and Pitarka (2010) broadband ground-  
412 motion simulation method. *Seismological Research Letters* 86(1): 75–80. DOI:10.1785/  
413 0220140101.
- 414 Graves RW and Pitarka A (2010) Broadband ground-motion simulation using a hybrid approach.  
415 *Bulletin of the Seismological Society of America* 100(5A): 2095–2123.
- 416 Hamburger R, Bonneville D, Crouse C, Dolan JD, Enfield B, Furr J, Hanson R, Harris JA, Heintz  
417 J, Holmes W, Hooper J, Kircher C, Luco N, McCabe S, Pekelnicky R, Siu J, Rezaeian  
418 S, Schneider P, Stewart JP, Sattar S, Tong M and Yuan J (2017) Development of the next  
419 generation of seismic design value maps for the 2020 NEHRP provisions. Other government  
420 series, National Institute of Building Sciences.
- 421 Jordan TH, Callaghan S, Graves RW, Wang F, Milner KR, Goulet CA, Maechling PJ, Olsen KB,  
422 Cui Y, Juve G, Vahi K, Yu J, Deelman E and Gill D (2018) CyberShake models of seismic  
423 hazards in southern and central California. In: *Proceedings of the US National Conference on*  
424 *Earthquake Engineering*. Los Angeles, California, USA: Earthquake Engineering Research  
425 Institute,.
- 426 LATBSDC (2008) *An Alternative Procedure for Seismic Analysis and Design of Tall Buildings*  
427 *Located in the Los Angeles Region*. Los Angeles Tall Buildings Structural Design Council

- 428 Los Angeles, CA.
- 429 Lee EJ and Chen P (2016) Improved basin structures in southern California obtained through full-  
430 3d seismic waveform tomography (F3DT). *Seismological Research Letters* 87(4): 874–881.  
431 DOI:10.1785/0220160013.
- 432 Moehle JP, Hamburger RO, Baker JW, Bray JD, Crouse CB, Deierlein GG, Hooper JD, Lew M,  
433 Maffei JR, Mahin SA, Malley J, Naeim F, Stewart JP and Wallace JW (2017) Guidelines  
434 for performance-based seismic design of tall buildings version 2.0. Technical Report PEER  
435 Report 2017/06, Berkeley, CA.
- 436 Petersen MD, Shumway AM, Powers PM, Mueller CS, Moschetti MP, Frankel AD, Rezaeian S,  
437 McNamara DE, Luco N, Boyd OS, Rukstales KS, Jaiswal KS, Thompson EM, Hoover SM,  
438 Clayton BS, Field EH and Zeng Y (2020) The 2018 update of the US national seismic hazard  
439 model: Overview of model and implications. *Earthquake Spectra* 36(1): 8755293019878199.  
440 DOI:10.1177/8755293019878199.
- 441 SCECpedia (2020) Accessing CyberShake seismograms. [https://SCEC.usc.edu/SCECpedia/Accessing\\_CyberShake](https://SCEC.usc.edu/SCECpedia/Accessing_CyberShake)
- 442 Shahi SK and Baker JW (2014) An efficient algorithm to identify strong-velocity pulses in  
443 multicomponent ground motions. *Bulletin of the Seismological Society of America* 104(5):  
444 2456–2466. DOI:10.1785/0120130191.
- 445 Small P, Gill D, Maechling PJ, Taborda R, Callaghan S, Jordan TH, Olsen KB, Ely GP and Goulet  
446 C (2017) The SCEC unified community velocity model software framework. *Seismological  
447 Research Letters* 88(6): 1539–1552. DOI:10.1785/0220170082.
- 448 Taborda R, Azizzadeh-Roodpish S, Khoshnevis N and Cheng K (2016) Evaluation of the southern  
449 California seismic velocity models through simulation of recorded events. *Geophysical  
450 Journal International* 205(3): 1342–1364. DOI:10.1093/gji/ggw085.
- 451 Teng G and Baker J (2019) Evaluation of SCEC CyberShake ground motions for engineering  
452 practice. *Earthquake Spectra* 35(3): 1311–1328. DOI:10.1193/100918EQS230M.